



Crystal structure of the N-terminal region of human Topoisomerase II β binding protein 1

Yan-gao Huo^{a,b}, Lin Bai^{a,b}, Min Xu^a, Tao Jiang^{a,*}

^a National Laboratory of Biomacromolecules, Institute of Biophysics, Chinese Academy of Sciences, 15 Datun Road, Chaoyang District, Beijing 100101, China

^b The Graduate University of Chinese Academy of Sciences, 19A Yuquan Road, Shijingshan District, Beijing 100039, China

ARTICLE INFO

Article history:

Received 6 September 2010

Available online 19 September 2010

Keywords:

Topoisomerase II β binding protein 1
BRCT domain
Crystal structure
Rad9
Checkpoint control

ABSTRACT

Human DNA Topoisomerase II β binding protein 1 (TopBP1) is a modulating protein that plays an essential role in the response to DNA damage. The N-terminal region of TopBP1, which contains predicted BRCA1-carboxy terminal (BRCT) domains 1 and 2, binds to Rad9, a component of the cell cycle checkpoint clamp Rad9-Hus1-Rad1 complex. Here, we report the crystal structure of the TopBP1 N-terminal region (residues 1–290) at 2.4 Å resolution. Interestingly, in addition to the predicted tandem BRCT1–2 repeats (residues 103–284), residues 7–98 form a previously unreported BRCT domain (here, BRCT0). In contrast to both BRCT1 and BRCT2, which possess the conventional phosphopeptide binding residues within a surface pocket, the corresponding pocket in BRCT0 is largely hydrophobic. Structural comparisons together with peptide binding studies indicate that the tandem BRCT1–2 domains are the binding region for phosphorylated Ser387 in Rad9.

© 2010 Elsevier Inc. All rights reserved.

1. Introduction

Cells utilize checkpoint control systems to recognize DNA lesions and suspend cell cycle progression until the damage is repaired. Replication Protein A (RPA), the Mre11-Rad50-Nbs1 (MRN) complex and the Rad9-Hus1-Rad1 (9-1-1) complex play key roles in the initial recognition of DNA lesions [1–4], and their cooperation with ATM or ATR, two phosphatidylinositol-3 kinase (PI3 K)-related protein kinases, elicits the activation of the DNA damage checkpoint [5,6].

Human DNA Topoisomerase II β binding protein 1 (TopBP1) contains eight BRCA1 carboxy-terminal (BRCT) domains and an ATR activation domain (AAD) located between the sixth and seventh BRCT domain [7]. Like its counterparts, Rad4/Cut5 in fission yeast and Dpb11 in budding yeast (reviewed in [8]), TopBP1 plays an essential role in bridging different protein partners that are involved in checkpoint control. For instance, TopBP1, the 9-1-1 complex and ATR are recruited to the site of certain types of DNA damage, after which the phosphorylated tail of Rad9 associates with the N-termi-

nal region of TopBP1, which contains its first two BRCT repeats. At the same time, the ATRIP/ATR complex can bind to the AAD domain of TopBP1, promoting the phosphorylation of Chk1 by ATR [9,10]. Moreover, previous studies have indicated that TopBP1 may have other partners that associate with its N-terminal region in response to DNA double-strand breaks, such as Nbs1, a key component of the Mre11-Rad50-Nbs1 (MRN) complex [11,12].

In addition to TopBP1, many other proteins in DNA damage response pathways are known to contain single or multiple BRCT domains. Crystal structures have been determined for many BRCT-containing proteins. The majority are in the form of tandem BRCT pairs such as in human BRCA1, MDC1, CRB2, BARD1 and LigIV [13–18]; while several are in the form of single BRCT domains like in XRCC1, Mcph1 and BRCT6 of TopBP1 [19–21]. These structures, in combination with biochemical studies, have revealed that tandem pairs of BRCT domains form a phospho-Ser/Thr binding module. The function of a single BRCT domain is less well characterized, but they are proposed to be involved in protein–protein interactions.

To better understand the structural and functional properties of TopBP1, we determined and analyzed the crystal structure of the N-terminal BRCT1–2 containing region of TopBP1 (TopBP1 N).

2. Materials and methods

2.1. Protein expression and purification

Human TopBP1 N (residues1–290) was expressed in *Escherichia coli* BL21 (DE3) at 16 °C for 18 h in LB medium from a pET-24a (+)

Abbreviations: TopBP1, Topoisomerase II β binding protein 1; TopBP1 N, TopBP1 N-terminus; BRCA1, breast cancer susceptibility gene 1; BRCT, BRCA1-carboxy terminal domain; Nbs1, Nijmegen breakage syndrome; ATM, ataxia-telangiectasia mutated protein kinase; ATR, ATM and Rad3-related; ATRIP, ATR-interacting protein; Chk1, checkpoint kinase 1; MDC1, DNA damage checkpoint protein 1; CRB2, Crumbs homolog 2; BARD1, BRCA1-associated RING domain protein 1; LigIV, DNA ligase IV; XRCC1, X-ray repair cross-complementing group 1; SPR, surface plasmon resonance.

* Corresponding author. Fax: +86 10 64888510.

E-mail address: tjiang@ibp.ac.cn (T. Jiang).

vector with a His₆-tag as its C-terminus. The harvested cell pellets were resuspended in lysis buffer (20 mM HEPES (pH 7.0), 300 mM NaCl, 5% glycerol (v/v), 0.1 mM PMSF, and 20 mM imidazole) and sonicated. The lysate was clarified by ultracentrifugation at 32,000 g for 40 min and purified on a nickel-affinity column containing 10 mL Chelating Sepharose Fast Flow matrix (GE Healthcare) followed by ion exchange chromatography using a 1 mL RESOURCETM S column (Amersham Pharmacia Biotech AB). Gel filtration was performed as the final purification step, using a Superdex 200 10/300 GL column (GE Healthcare) in a buffer containing 50 mM sodium acetate (pH 5.6), 200 mM NaCl, 4 mM DTT, and 2 mM EDTA. The protein was concentrated to 8 mg/mL for crystallization. SeMet-substituted TopBP1 N was overexpressed as previously described [22] and purified as above.

2.2. Crystallization

Single crystals of TopBP1 N were grown at 16 °C using hanging drop vapor diffusion method by mixing 1 μL protein solution with 1 μL reservoir solution A (11% PEG3350 (w/v), 0.1 M MES (pH 5.5), 0.85 M NaNO₃, 4 mM DTT, and 2 mM EDTA). The SeMet-TopBP1 N single crystals were grown under the same conditions. Because the resolution obtained from initial crystals was low (10 Å), a dehydration procedure was introduced. Reservoir solution A was exchanged into solution B [30% PEG3350(w/v), 0.1 M MES(pH5.5), 0.85 M NaNO₃, 4 mM DTT, and 2 mM EDTA] for 12–16 h, the crystals were then looped out and soaked into reservoir solution B plus 15% sucrose (w/v) for approximately 10 min and subsequently flash cooled in liquid nitrogen for data collection.

2.3. Data collection and structure determination

SeMet-TopBP1 N diffraction data were collected at beamline 17U (BL17U) at the Shanghai Synchrotron Radiation Facility (SSRF) and processed with HKL2000 [23]. The initial phases were obtained using single-wavelength anomalous dispersion method and the program PHENIX [24]. The molecular model was built with Coot [25] and refined with REFMAC [26]. The final model was refined to an R-factor of 22.4% and a free-R factor of 25.3% (Table 1). Figures were produced with PyMOL (<http://www.pymol.org/>).

2.4. Biacore analysis

TopBP1 BRCT1–2 (residues 99–290) was expressed from vector pET-24a(+) as a C-terminal His₆-tagged protein in *Escherichia coli* BL21 (DE3) at 16 °C. After nickel affinity chromatography, the protein was purified on a Superdex 200 10/300 GL column (GE Healthcare) in a buffer containing 20 mM HEPES (pH 7.5), and 200 mM NaCl. A phosphorylated-Ser387-containing peptide derived from the C-terminal tail of Rad9 (sequence: 380-SPVLAED(pS)EGEG-391, referred to as Rad9-pSer387-tail peptide below) was purchased from Chinapeptides Co., Ltd. (Shanghai, CHN). Binding assays between the Rad9-pSer387-tail peptide and BRCT 0–2 or BRCT 1–2 were carried out using a Biacore 3000 instrument (GE Healthcare, Uppsala, Sweden). Purified BRCT0–2 and BRCT1–2 were immobilized on different channels of a CM5 chip (GE Healthcare) using an amine coupling kit to a target of 5100 and 3400 response units (Ru), respectively; this ensured that the number of molecules immobilized on the chip were approximately equal for each protein. The remaining uncoupled sites were blocked with 1 M ethanolamine at pH 8.5. Three concentrations of Rad9-pSer387-tail peptide (0.8 mM, 1.6 mM, and 2.0 mM) dissolved in binding buffer (140 mM NaCl, 2.7 mM KCl, 10 mM Na₂HPO₄, and 1.8 mM KH₂PO₄, 0.005% Tween-20, pH 7.3) were tested. All assays were performed at 25 °C and the data were analyzed with BIAevaluation software version 4.1.

Table 1
Data collection, structure determination, and refinement statistics.

Crystallographic statistics	
Space group	P2 ₁ 3
Cell parameters (Å, °)	a = b = c = 115.73, α = β = γ = 90
Resolution (Å)	50–2.4
Reflections (total/unique)	966790(20531)
Completeness (%)	100
R _{merge} ^a	0.078(0.409)
Molecular model refinement	–
R factors	–
R _{cryst} ^b	0.224
R _{free} ^c	0.253
R.m.s.d. values	–
Bond lengths (Å)	0.0118
Bond angles (°)	1.291
B factor (Å ²)	42.115
Main chain (Å ²)	40.823
Side chain (Å ²)	43.307
Ramachandran plot statistics	–
Favored regions	92.9%
Allowed regions	7.1%
Outlier regions	0

^a $R_{merge} = \frac{\sum_{hkl} \sum_i |I_{hkl,i} - \langle I_{hkl} \rangle|}{\sum_{hkl} \sum_i I_{hkl,i}}$ where I_{hkl} is the intensity of a reflection and $\langle I_{hkl} \rangle$ is the average of all observations of this reflection and its symmetry equivalents.

^b $R_{cryst} = \frac{\sum ||F_{obs}| - |F_{calc}||}{\sum |F_{obs}|}$, where F_{obs} and F_{calc} are the observed and calculated structure factor amplitudes, respectively.

^c R_{free} as R_{cryst}, but calculated from 10% of the data excluded from the refinement.

3. Results and discussion

3.1. Overall structure

The crystal structure of TopBP1 N (encompassing residues 1–290) was determined at 2.4 Å resolution with single-wavelength anomalous diffraction (SAD) phasing method. The final model contains one molecule in the asymmetric unit with residues 7–284 built in. The statistics from data collection and processing are presented in Table 1. The PDB ID of the refined structure is 3OLC.

The overall structure of TopBP1 N resembles an elongated cylinder containing three domains. Interestingly, in addition to the previously predicted BRCT domains (BRCT1, residues 103–197; and BRCT2, residues 203–284), residues 7–98 also form a BRCT domain, which consists of a central four-stranded parallel β-sheet surrounded by four α-helices. Thus, we refer to these three domains in sequence as BRCT0, 1 and 2 (Fig. 1A). Superposition of the three domains reveals that the RMSD for the C_α atoms are 2.5 Å between BRCT0 and BRCT1, 2.9 Å between BRCT0 and BRCT2, and 1.8 Å between BRCT1 and BRCT2.

It has been shown in previous studies that the tandem BRCT repeats function as phosphopeptide-binding modules, in which the substrate binding pocket consists of two key regions: a phosphoserine (pSer) recognition surface pocket in the first BRCT and a hydrophobic specificity cleft between the two BRCT domains [13–15,27]. The superposition of BRCT1–2 from TopBP1 N with the tandem pair of BRCT domains of either BRCA1 (PDB ID: 1T15) or NBS1 (PDB ID: 3HUE) reveals that the relative orientations of BRCT1 and 2 in TopBP1 N are largely different from the relative orientations of the BRCT domains of BRCA1 and NBS1, suggesting the dynamic nature of the tandem domains (Fig. 1B).

3.2. Surface pocket of the three BRCT domains

In BRCA1, residues S1655 and K1702 in the surface pocket mediate pSer/pThr binding [27]. Therefore, we examined the corresponding region of the three TopBP1 BRCT domains. The corresponding residues in BRCT 1 and 2 are T114/K155, T208/K250, respectively, which are compatible in with phosphate binding. In

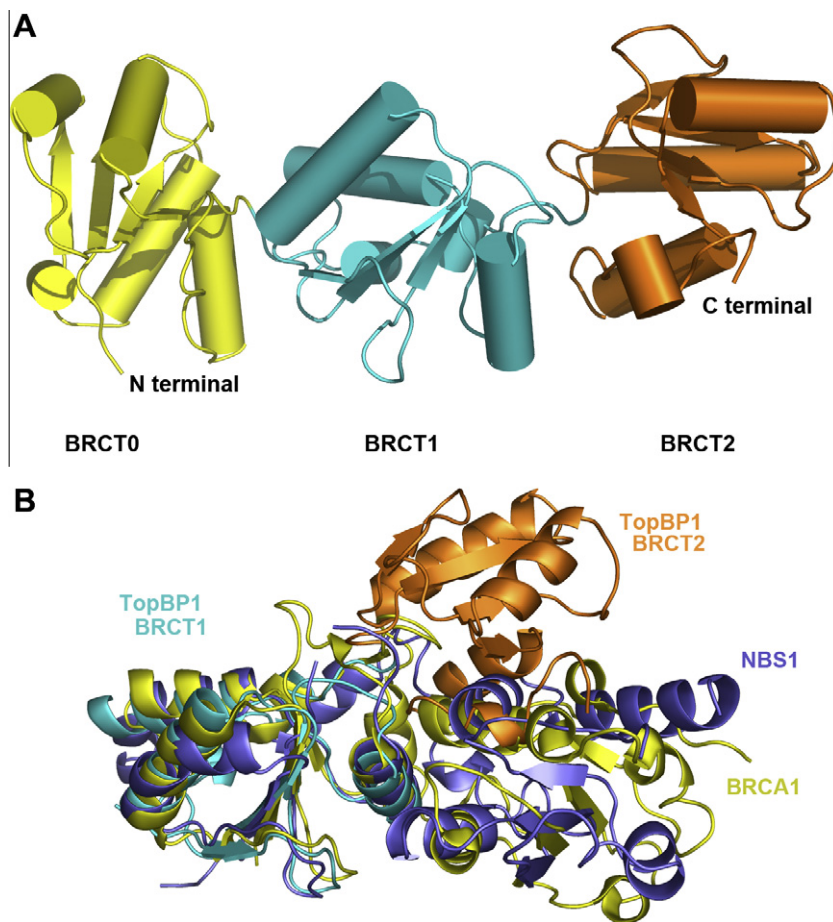


Fig. 1. (A). Overall ribbon structure of TopBP1 N. TopBP1 N contains three independent sandwich-like BRCT domains (BRCT0 (yellow), BRCT1 (cyan), BRCT2 (orange)). (B). Superposition of BRCT1 (cyan) and BRCT2 (orange) from TopBP1 with BRCT domains from BRCA1 (yellow) and NBS1 (blue), indicating that the relative orientations of BRCT1 and 2 are largely different from those of BRCA1 and NBS1. (For interpretation of the references to color in this figure legend, the reader is referred to the web version of this article.)

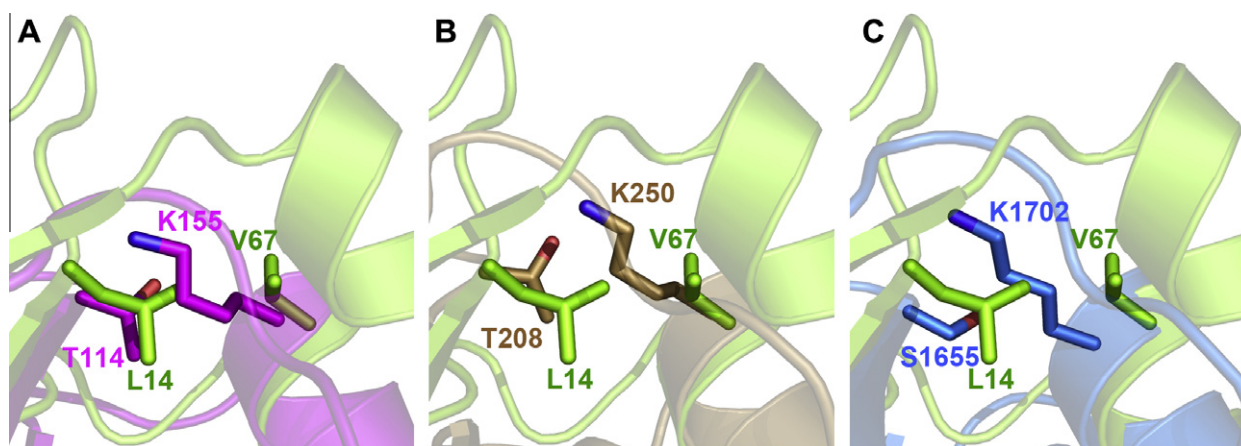


Fig. 2. Structural alignments of the binding pockets of BRCT0 (green), BRCT1 (magenta), BRCT2 (brown) and BRCA1 (aquamarine). (For interpretation of the references to color in this figure legend, the reader is referred to the web version of this article.)

BRCT0, the corresponding residues are hydrophobic (L14 and V67), suggesting the absence of a phosphopeptide binding pocket (Fig. 2).

Previous crystal structure studies have revealed that, in contrast to tandem BRCT repeats, single BRCT domains may have functions other than phosphopeptide binding. For instance, human Mcph1 (also known as BRIT1) is a 92.7 kD modulating protein that

contains a single BRCT domain at its N-terminus (Mcph1 N) and a tandem pair of BRCT domains at its C-terminus. The crystal structure of Mcph1 N (PDB ID: 2WT8) reveals that the typical phosphoserine (pSer) interacting residues (S1655 and K1702 in BRCA1) have been replaced by E14 and T59, respectively. These two residues, together with the adjacent hydrophobic residues W16 and Y56, form a surface pocket that is proposed to be involved in

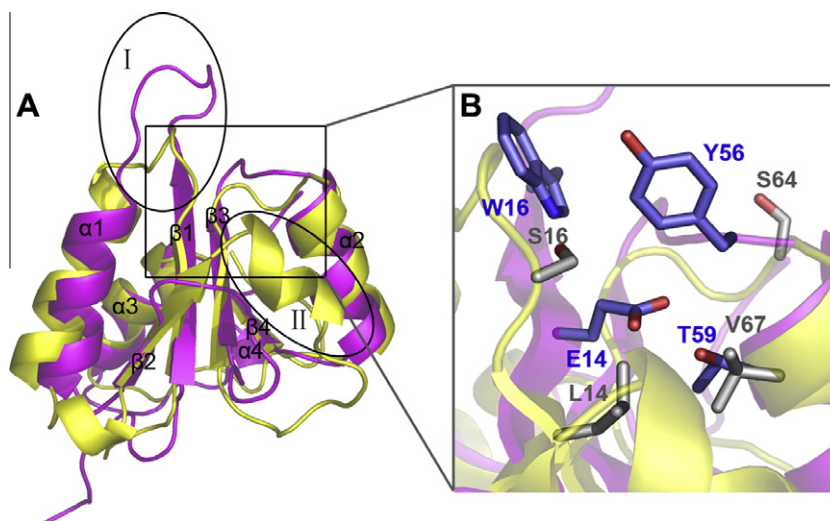


Fig. 3. (A) Superposition of BRCT0 (yellow) and Mcph1 N (magenta). The major differences are highlighted with ovals (I and II). (B) Close-up view of the surface pocket. Residues from BRCT0 are shown in gray and residues from Mcph1 are shown in blue. (For interpretation of the references to color in this figure legend, the reader is referred to the web version of this article.)

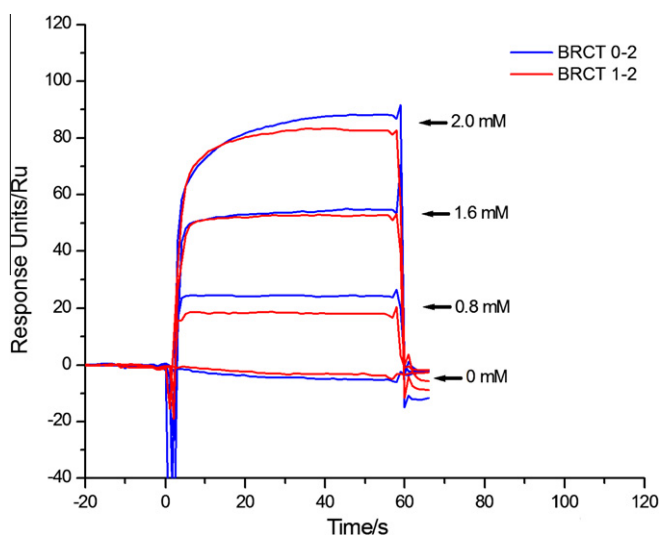


Fig. 4. Biacore binding assays of the phosphorylated-Ser387-containing peptide [380-SPVLAED(p-S)EGEG-391] from Rad9 to BRCT0-2 (blue) and BRCT 1-2 (red) from the N-terminal region of TopBP1. Three concentrations of the peptide were measured. The results suggest that the absence of BRCT0 only slightly reduces the binding affinity between TopBP1 N and the phosphopeptide. (For interpretation of the references to color in this figure legend, the reader is referred to the web version of this article.)

protein–protein interaction and necessary to prevent abnormal chromosome condensation [20]. We speculate that BRCT0 of TopBP1 N may also function in protein–protein interactions.

To further investigate this possibility, we superposed BRCT0 with Mcph1 N. The superposition reveals several remarkable differences between the two structures. First, the two bulky residues W16 and Y56 in the surface pocket of Mcph1 are replaced by two Serines (S16 and S64, respectively) in BRCT0. Second, the loop between β1 and α1 in Mcph1 is much longer than that in BRCT0. Third, the loop connecting β2 and β3 in Mcph1 is substituted by a short alpha helix in BRCT0 (Fig. 3). Given that the last two differences occur at positions adjacent to the surface pocket, we speculate that they may contribute to the binding specificity of BRCT0. However, further investigation will be required for a full understanding of the function of BRCT0.

3.3. Peptide binding assays

In response to DNA damage, the 9-1-1 complex can be loaded onto DNA lesion sites by Rad17-RFC2-5 to activate the cell cycle checkpoint [28]. Previous studies have confirmed that the N-terminal domain of Rad9 (270 amino acids) associates with Hus1 and Rad1, and that its heavily phosphorylated C-terminus participates in association with other proteins including TopBP1. The C-terminal tail of Rad9 is phosphorylated at multiple sites, including Ser272, Ser277, Thr292, Ser328, Ser336, Ser341, Thr355, Ser375, Ser380 and Ser387. However, it has been reported that the phosphorylation of Ser387 is required for the interaction between Rad9 and the N-terminal region of TopBP1 [7,10,29–31].

To better understand the interaction between the TopBP1 N-terminus and Rad9, we constructed a truncated form of TopBP1 N that contains only BRCT1–2 (residues 99–290), and performed a SPR experiment to measure the binding affinities between a phosphorylated Ser387-containing peptide derived from the tail of Rad9 (the Rad9-pSer387-tail peptide) and BRCT0–2 or BRCT1–2. Our results indicate that the loss of BRCT0 only slightly reduces the binding affinity of TopBP1 N for the Rad9-pSer387-tail peptide (Fig. 4), which is consistent with our structure-driven hypothesis that BRCT1 and 2 form the binding sites for the phosphorylated peptide.

4. Conclusions

In summary, the structure of the N-terminus of TopBP1 reveals that it contains previously undocumented three tandem BRCT domains. Future work will aim to identify additional proteins that bind to this region and define the structural and functional importance of these interactions. We expect that the structural insights gained from this work will aid the design of specific TopBP1 inhibitors, which may be used to selectively regulate the cell cycle checkpoint.

5. Addendum

During the preparation of this manuscript, an article on the crystal structure of the same region of TopBP1 was published online [32].

Acknowledgments

We would like to thank the staff at the Shanghai Synchrotron Radiation Facility (SSRF) and K.Q. Ye for assistance in data collection. We would also like to thank Y. Y. Chen for performing the Biacore analysis. This research was financially supported by The National Key Basic Research Program (Grant 2006CB910902, 2011CB910302), The National Natural Science Foundation of China (Grants 30770435, 30721003), and The National High Technology Research and Development Program of China (Grant 2006AA02A319).

References

- [1] J. Bartek, C. Lukas, J. Lukas, Checking on DNA damage in S phase, *Nat. Rev. Mol. Cell. Biol.* 5 (2004) 792–804.
- [2] P. Roos-Mattjus, B.T. Vroman, M.A. Burtelow, M. Rauen, A.K. Eapen, L.M. Karnitz, Genotoxin-induced Rad9-Hus1-Rad1 (9-1-1) chromatin association is an early checkpoint signaling event, *J. Biol. Chem.* 277 (2002) 43809–43812.
- [3] Y. Zou, Y. Liu, X. Wu, S.M. Shell, Functions of human replication protein A (RPA): from DNA replication to DNA damage and stress responses, *J. Cell. Physiol.* 208 (2006) 267–273.
- [4] E. Olson, C.J. Nievera, A.Y. Lee, L. Chen, X. Wu, The Mre11-Rad50-Nbs1 complex acts both upstream and downstream of ataxia telangiectasia mutated and Rad3-related protein (ATR) to regulate the S-phase checkpoint following UV treatment, *J. Biol. Chem.* 282 (2007) 22939–22952.
- [5] A. Dupre, L. Boyer-Chatenet, J. Gautier, Two-step activation of ATM by DNA and the Mre11-Rad50-Nbs1 complex, *Nat. Struct. Mol. Biol.* 13 (2006) 451–457.
- [6] J.H. Lee, T.T. Paull, ATM activation by DNA double-strand breaks through the Mre11-Rad50-Nbs1 complex, *Science* 308 (2005) 551–554.
- [7] S. Delacroix, J.M. Wagner, M. Kobayashi, K. Yamamoto, L.M. Karnitz, The Rad9-Hus1-Rad1 (9-1-1) clamp activates checkpoint signaling via TopBP1, *Genes Dev.* 21 (2007) 1472–1477.
- [8] V. Garcia, K. Furuya, A.M. Carr, Identification and functional analysis of TopBP1 and its homologs, *DNA Repair (Amst)* 4 (2005) 1227–1239.
- [9] Y. Hashimoto, T. Tsujimura, A. Sugino, H. Takisawa, The phosphorylated C-terminal domain of *Xenopus* Cut5 directly mediates ATR-dependent activation of Chk1, *Genes Cells* 11 (2006) 993–1007.
- [10] J. Lee, A. Kumagai, W.G. Dunphy, The Rad9-Hus1-Rad1 checkpoint clamp regulates interaction of TopBP1 with ATR, *J Biol Chem* 282 (2007) 28036–28044.
- [11] H.Y. Yoo, A. Kumagai, A. Shevchenko, A. Shevchenko, W.G. Dunphy, The Mre11-Rad50-Nbs1 complex mediates activation of TopBP1 by ATM, *Mol. Biol. Cell* 20 (2009) 2351–2360.
- [12] K. Morishima, S. Sakamoto, J. Kobayashi, H. Izumi, T. Suda, Y. Matsumoto, H. Tauchi, H. Ide, K. Komatsu, S. Matsuura, TopBP1 associates with NBS1 and is involved in homologous recombination repair, *Biochem. Biophys. Res. Commun.* 362 (2007) 872–879.
- [13] J.A. Clapperton, I.A. Manke, D.M. Lowery, T. Ho, L.F. Haire, M.B. Yaffe, S.J. Smerdon, Structure and mechanism of BRCA1 BRCT domain recognition of phosphorylated BACH1 with implications for cancer, *Nat. Struct. Mol. Biol.* 11 (2004) 512–518.
- [14] Y. Shen, L. Tong, Structural evidence for direct interactions between the BRCT domains of human BRCA1 and a phospho-peptide from human ACC1, *Biochemistry* 47 (2008) 5767–5773.
- [15] M.S. Lee, R.A. Edwards, G.L. Thede, J.N. Glover, Structure of the BRCT repeat domain of MDC1 and its specificity for the free COOH-terminal end of the gamma-H2AX histone tail, *J. Biol. Chem.* 280 (2005) 32053–32056.
- [16] M.L. Kilkenny, A.S. Dore, S.M. Roe, K. Nestoras, J.C. Ho, F.Z. Watts, L.H. Pearl, Structural and functional analysis of the Crb2-BRCT2 domain reveals distinct roles in checkpoint signaling and DNA damage repair, *Genes Dev.* 22 (2008) 2034–2047.
- [17] G. Birrane, A.K. Varma, A. Soni, J.A. Ladias, Crystal structure of the BARD1 BRCT domains, *Biochemistry* 46 (2007) 7706–7712.
- [18] P.Y. Wu, P. Frit, S. Meesala, S. Dauvillier, M. Modesti, S.N. Andres, Y. Huang, J. Sekiguchi, P. Calsou, B. Salles, M.S. Junop, Structural and functional interaction between the human DNA repair proteins DNA ligase IV and XRCC4, *Mol. Cell. Biol.* 29 (2009) 3163–3172.
- [19] X. Zhang, S. Morera, P.A. Bates, P.C. Whitehead, A.I. Coffey, K. Hainbucher, R.A. Nash, M.J. Sternberg, T. Lindahl, P.S. Freemont, Structure of an XRCC1 BRCT domain: a new protein-protein interaction module, *Embo J.* 17 (1998) 6404–6411.
- [20] M.W. Richards, J.W. Leung, S.M. Roe, K. Li, J. Chen, R. Bayliss, A pocket on the surface of the N-terminal BRCT domain of Mcp1 is required to prevent abnormal chromosome condensation, *J. Mol. Biol.* 395 (2010) 908–915.
- [21] C.C. Leung, E. Kellogg, A. Kuhnert, F. Hanel, D. Baker, J.N. Glover, Insights from the crystal structure of the sixth BRCT domain of topoisomerase IIbeta binding protein 1, *Protein Sci.* 19 (2010) 162–167.
- [22] S. Double, Production of selenomethionyl proteins in prokaryotic and eukaryotic expression systems, *Methods Mol. Biol.* 363 (2007) 91–108.
- [23] Z. Otwinowski, W. Minor, Processing of X-ray diffraction data collected in oscillation mode, *Methods Enzymol.* 276 (1997) 307–326.
- [24] P.D. Adams, R.W. Grosse-Kunstleve, L.W. Hung, T.R. Ioerger, A.J. McCoy, N.W. Moriarty, R.J. Read, J.C. Sacchettini, N.K. Sauter, T.C. Terwilliger, PHENIX: building new software for automated crystallographic structure determination, *Acta Crystallogr., Sect. D: Biol. Crystallogr.* 58 (2002) 1948–1954.
- [25] P. Emsley, K. Cowtan, Coot: model-building tools for molecular graphics, *Acta Crystallogr., sect. D: Biol. Crystallogr.* 60 (2004) 2126–2132.
- [26] G.N. Murshudov, A.A. Vagin, E.J. Dodson, Refinement of macromolecular structures by the maximum-likelihood method, *Acta Crystallogr., sect. D: Biol. Crystallogr.* 53 (1997) 240–255.
- [27] S.J. Campbell, R.A. Edwards, J.N. Glover, Comparison of the structures and peptide binding specificities of the BRCT domains of MDC1 and BRCA1, *Structure* 18 (2010) 167–176.
- [28] L. Zou, D. Cortez, S.J. Elledge, Regulation of ATR substrate selection by Rad17-dependent loading of Rad9 complexes onto chromatin, *Genes Dev.* 16 (2002) 198–208.
- [29] P. Roos-Mattjus, K.M. Hopkins, A.J. Oestreich, B.T. Vroman, K.L. Johnson, S. Naylor, H.B. Lieberman, L.M. Karnitz, Phosphorylation of human Rad9 is required for genotoxin-activated checkpoint signaling, *J. Biol. Chem.* 278 (2003) 24428–24437.
- [30] R.P. St Onge, B.D. Besley, J.L. Pelley, S. Davey, A role for the phosphorylation of hRad9 in checkpoint signaling, *J. Biol. Chem.* 278 (2003) 26620–26628.
- [31] Y. Takeishi, E. Ohashi, K. Ogawa, H. Masai, C. Obuse, T. Tsurimoto, Casein kinase 2-dependent phosphorylation of human Rad9 mediates the interaction between human Rad9-Hus1-Rad1 complex and TopBP1, *Genes Cells* 15 (2010) 761–771.
- [32] M. Rappas, A.W. Oliver, L.H. Pearl, Structure and function of the Rad9-binding region of the DNA-damage checkpoint adaptor TopBP1, *Nucleic Acids Res.* (2010).